

Clinical and molecular characterization of steatotic liver disease in the setting of immune-mediated inflammatory diseases

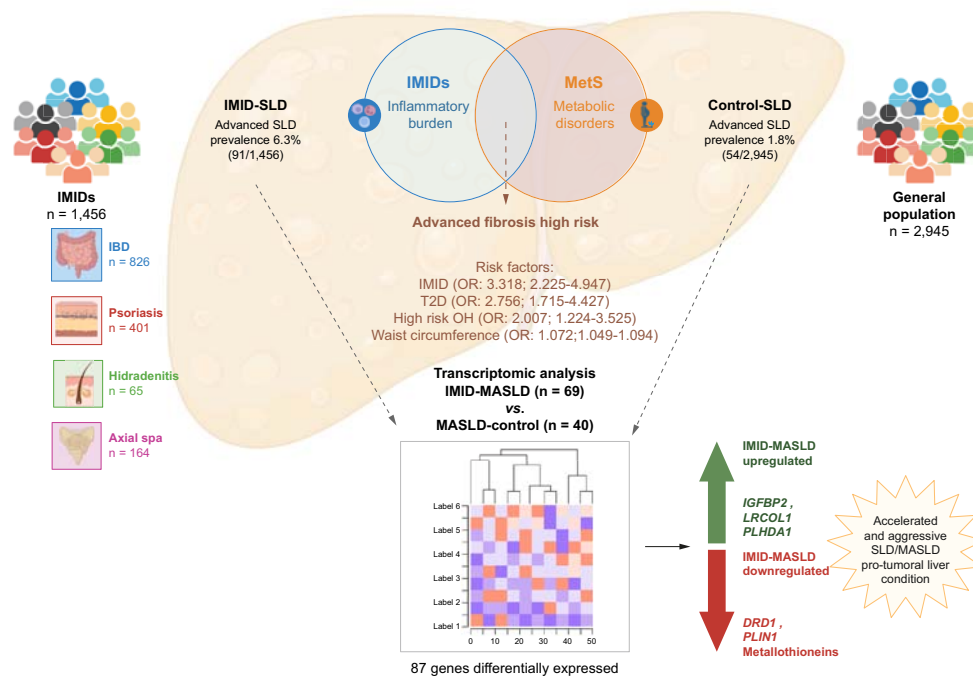
Authors

Enrique García-Nieto, Juan Carlos Rodríguez-Duque, Coral Rivas-Rivas, ..., Jose Pedro Vaque, Javier Crespo, María Teresa Arias-Loste

Correspondence

ariasloste@gmail.com, mteresa.arias@scsalud.es (M.T. Arias-Loste), javier.crespo@scsalud.es (J. Crespo).

Graphical abstract



Highlights:

- The prevalence of advanced SLD and MASLD is markedly higher in patients with IMID than in the general population.
- Patients with IMID and advanced stages of SLD/MASLD were younger with a lower prevalence of T2D and hazardous alcohol consumption.
- An increased prevalence of cryptogenic SLD in patients with IMID points to a distinct and specific etiology.
- Transcriptome analysis identified 87 genes with significant differential expression between patients with IMID-MASLD and controls.

Impact and implications:

The prevalence of steatotic liver disease with advanced fibrosis is increased in patients with immune-mediated inflammatory diseases, independent of classic metabolic risk factors or high-risk alcohol consumption. Transcriptomic analysis revealed a unique gene expression signature associated with cellular activities that are compatible with a liver condition leading to an accelerated and aggressive form of steatotic liver disease. Our findings underscore the importance of heightened screening for advanced liver disease risk across various medical disciplines overseeing patients with immune-mediated inflammatory diseases.

Clinical and molecular characterization of steatotic liver disease in the setting of immune-mediated inflammatory diseases

Enrique García-Nieto^{1,†}, Juan Carlos Rodríguez-Duque^{1,2,†}, Coral Rivas-Rivas^{1,2}, Paula Iruzubieta^{1,2}, María José García^{1,2}, Laura Rasines¹, Ana Alvarez-Cancelo¹, Agustín García-Blanco¹, José Ignacio Fortea^{1,2}, Angela Puente^{1,2}, Beatriz Castro^{1,2}, María Luisa Cagigal³, Javier Rueda-Gotor⁴, Ricardo Blanco⁴, Montserrat Rivero^{1,2}, Susana Armesto⁵, Marcos Antonio González-López⁵, Anna Esteve Codina⁶, Marta Gut⁶, Jose Pedro Vaque^{1,7,‡}, Javier Crespo^{1,2,*,‡}, María Teresa Arias-Loste^{1,2,*,‡}

JHEP Reports 2024. vol. 6 | 1–13



Background & Aims: Growing evidence suggests an increased prevalence of metabolic dysfunction-associated steatotic liver disease (MASLD) in the context of immune-mediated inflammatory diseases (IMIDs). We aimed to clinically and mechanistically characterize steatotic liver disease (SLD) in a prospective cohort of patients with IMID compared to controls.

Methods: Cross-sectional, case-control study including a subset of patients with IMID. Controls from the general population were age-, sex-, type 2 diabetes-, and BMI-matched at a 1:2 ratio. SLD was established using controlled attenuation parameter. Liver biopsies were obtained when significant liver fibrosis was suspected. Total RNA was extracted from freshly frozen cases and analyzed by RNA-seq. Differential gene expression was performed with 'limma-voom'. Gene set-enrichment analysis was performed using the fgsea R package with a preranked "limma t-statistic" gene list.

Results: A total of 1,456 patients with IMID and 2,945 controls were included. Advanced SLD (liver stiffness measurement ≥ 9.7 kPa) (13.46% vs. 3.79%; $p < 0.001$) and advanced MASLD (12.8% vs. 2.8%; $p < 0.001$) prevalence were significantly higher among patients with IMID than controls. In multivariate analysis, concomitant IMID was an independent, and the strongest, predictor of advanced SLD (adjusted odds ratio 3.318; 95% CI 2.225–4.947; $p < 0.001$). Transcriptomic data was obtained in 109 patients and showed 87 significant genes differentially expressed between IMID-MASLD and control-MASLD. IMID-MASLD cases displayed an enriched expression of genes implicated in pro-tumoral activities or the control of the cell cycle concomitant with a negative expression of genes related to metabolism.

Conclusions: The prevalence of advanced SLD and MASLD is disproportionately elevated in IMID cohorts. Our findings suggest that IMIDs may catalyze a distinct MASLD pathway, divergent from classical metabolic routes, highlighting the need for tailored clinical management strategies.

© 2024 The Authors. Published by Elsevier B.V. on behalf of European Association for the Study of the Liver (EASL). This is an open access article under the CC BY-NC-ND license (<http://creativecommons.org/licenses/by-nc-nd/4.0/>).

Introduction

In the past few decades, metabolic dysfunction-associated steatotic liver disease (MASLD) has ascended to become the predominant chronic liver pathology globally,¹ its incidence mirroring the upward trends in obesity and type 2 diabetes (T2D) – its principal risk factors.^{2,3} The hepatic deposition of fat epitomizes a systemic metabolic dysregulation, portending potential progression to metabolic dysfunction-associated steatohepatitis (MASH), liver fibrosis, cirrhotic decompensation, and hepatocellular carcinoma (HCC).⁴ Despite the clear association with metabolic anomalies, MASLD exhibits remarkable heterogeneity in phenotypic expression, progression rates, and prognostic outcomes. This variability is

underscored by MASLD's manifestation in normoweight individuals devoid of overt insulin resistance or T2D.⁵

Our research collective has identified an elevated MASLD and advanced liver fibrosis proclivity in individuals with immune-mediated inflammatory diseases (IMIDs), such as inflammatory bowel disease (IBD)⁶ and hidradenitis suppurativa.⁷ This susceptibility appears independent from the classical metabolic risk parameters. IMIDs constitute a diverse array of prevalent, chronic disorders including IBD, psoriasis/psoriatic arthritis, rheumatoid arthritis, and ankylosing spondylitis. These conditions are unified by shared etiopathogenic pathways, invoking a complex nexus of genetic predisposition – highlighted by their epidemiological co-occurrence and familial

* Corresponding authors. Address: Servicio de Aparato Digestivo, Hospital Universitario Marqués de Valdecilla, Avda. Valdecilla n° 25, 39008 Santander, Spain; Tel.: +34 942 202520.

E-mail addresses: ariasloste@gmail.com, mteresa.arias@scsalud.es (M.T. Arias-Loste), javier.crespo@scsalud.es (J. Crespo).

† Authors contributed equally to this manuscript.

‡ Authors jointly supervised this work and share seniorship.

<https://doi.org/10.1016/j.jhepr.2024.101167>



agglomeration – and environmental precipitants that instigate aberrant immune responses and proinflammatory cytokine imbalance.⁸ While the IMID phenotype is defined by the afflicted organ, such as the intestines in IBD or the skin in psoriasis, patients are concurrently at heightened risk for comorbidities as a direct sequela of persistent inflammation.⁹

Our hypothesis posits that patients with IMID are predisposed to developing steatotic liver disease (SLD), irrespective of the traditional metabolic risk factors, possibly exhibiting a unique hepatic molecular signature driven by the chronic inflammatory milieu. Our aim is to delineate the clinical and mechanistic profiles of a prospective cohort of patients with IMID-associated SLD and compare these findings with those in patients presenting with SLD of a metabolic origin.

Materials and methods

Study design and participants

We performed a cross-sectional, case-control study ([ClinicalTrials.gov](https://clinicaltrials.gov/ct2/show/study/NCT03760172) Identifier: NCT03760172). This study included a multicohort of consecutive patients with IMIDs, including IBD, psoriasis, hidradenitis suppurativa and axial spondyloarthritis. Patients attended the Gastroenterology, Dermatology, and Rheumatology outpatient clinics of the University Hospital Marques de Valdecilla (HUMV) in Santander between December 2018 and December 2019. The inclusion criteria for participation in the study were defined as follows: age ≥ 18 years-old, provided written informed consent, and present with a reliable transient elastography (TE) assessment (consisting of at least 10 valid measurements, a success rate of over 60%, and low variability as evidenced by an IQR of less than 0.3). Patients who had any clinical evidence of malignancy or other secondary causes of chronic liver disease were excluded.

A random sample of individuals from the general population, stemming from the Spanish Hepatitis C Prevalence Study ([ClinicalTrials.gov](https://clinicaltrials.gov/ct2/show/study/NCT02749864) Identifier: NCT02749864),¹⁰ was included as a control group. Those with secondary causes of liver disease were excluded, as were individuals with concomitant diagnoses of IMID. Patients and controls were matched by age, sex, T2D, and BMI in a 1:2 ratio.

Additionally, a secondary control group was formed from a sample of a real-world cohort of patients with biopsy-proven MASLD who attended MASLD outpatient clinics at HUMV. HUMV is a referral centre for liver diseases, and MASLD liver biopsies comprised of samples obtained in clinical practice mainly on occasions when the results obtained from TE gave rise to a suspicion of MASH and/or advanced liver fibrosis.¹¹ Patients with a known diagnosis of IMID were excluded from this group to enable comparisons of the clinical and histological characteristics of patients with “classic MASLD” (control-MASLD) with those of patients with MASLD arising in an IMID setting (IMID-MASLD). Patients with biopsy-proven IMID-MASLD were paired with patients with biopsy-proven control-MASLD by age and grade of liver fibrosis in a 1:2 ratio and constituted our translational study cohort (TSC).

Written informed consent was obtained from all patients and controls, and the study was conducted in accordance with the ethical guidelines of the Declaration of Helsinki and with the approval of the local Ethics Committees (CEIC-Cantabria. Code: 2018.139).

Clinical evaluation and laboratory collection

Anthropometric data were collected from all participants at inclusion to calculate their BMI and waist circumference. Information regarding smoking status, self-reported alcohol consumption, concomitant presence of classic cardiovascular risk factors, and the use of potential hepatotoxic medications was collected during clinical interviews.

In patients with IMID, information about the disease phenotype, duration, activity, complications, and past and current treatments was prospectively and systematically collected. Fasting venous blood samples were collected at inclusion.

Diagnosis of SLD

A controlled attenuation parameter (CAP® - Echosens; Paris, France) measured using TE was used to diagnose and quantify hepatic steatosis. The cut-off value used to determine the presence of SLD was 248 dB/m for $>S_0$.¹² After this determination, patients were categorised as having MASLD, metabolic and high-risk alcohol-associated liver disease (MetALD), or other etiologies/cryptogenic SLD, adhering to the nomenclature recently proposed.¹³ High-risk alcohol consumption was defined as an intake exceeding 20 g daily in women and 30 g daily in men.

Liver fibrosis and histology assessment

All participants had their extent of liver fibrosis estimated by TE (FibroScan® - Echosens; Paris, France). Experienced hepatologists performed all examinations following the manufacturer's recommendations. Significant liver fibrosis was indicated by values ≥ 7.2 kPa, while values ≥ 9.7 kPa indicated advanced liver fibrosis (advanced SLD or MASLD).¹⁴ The findings suggestive of advanced fibrosis were corroborated in a second elastography assessment.

Liver biopsies were obtained percutaneously with a Tru-Cut biopsy needle following a standard procedure in patients with suspected significant liver fibrosis according to liver stiffness measurement (LSM). Liver biopsy specimens of at least 2.0 cm (≥ 10 portal tracts) in length obtained with a 16-gauge cutting needle were included. Samples were digitalized and reviewed by a single expert pathologist unaware of the clinical findings. Four histological features (steatosis, lobular inflammation, hepatocellular ballooning, and fibrosis) were evaluated according to the activity score and staging system devised by the Pathology Committee of the NASH Clinical Research Network.

Total RNA extraction and RNA-seq data processing

Total RNA was extracted from freshly frozen biopsies. Freshly frozen biopsies were disrupted using a Kimble® Pellet Pestle® Cordless Motor (DWK Life Sciences, Cat. No.: 749540-0000). RNA extraction was performed using the PureLink™ RNA Mini Kit (Invitrogen, Cat. No.: 12183018A) adding an extra purification process with the PureLink™ DNase Set (Invitrogen, Cat. No.: 12185010). RNA quality was analyzed using RNA ScreenTape (Agilent). Samples were required to have a minimum RNA integrity number >8 .

RNA-seq reads were mapped against the human reference genome (GRCh38) using STAR (version 2.5.3a)¹⁵ with ENCODE parameters. Genes were quantified using RSEM (version

1.3.0)¹⁶ with default parameters. The human gene annotation file was downloaded from gencode release 36 (<https://www.gencodegenes.org/>). Mapping and quantification quality checking were performed with GEMTools (<https://gemtools.github.io/>) and custom python scripts. A multidimensional scaling plot was performed to inspect sample similarities using the ‘voom’ transformed counts and the top 500 most variable genes. Differential gene expression was performed with ‘limma-voom’¹⁷ adjusting for BMI, sex, and fibrosis severity in the model. Genes with a false discovery rate <5% were considered differentially expressed. Gene set-enrichment analysis was performed with the fgsea R package¹⁸ with a preranked “limma t-statistic” gene list. A heatmap plot with the differentially expressed genes was generated with the R package pheatmap with the scale = ‘row’ options and voom transformed counts.

Serum IGFBP-2 evaluation

Since *IGFBP2* was the top hit expressed gene in IMID-MASLD liver biopsies, serum IGFBP-2 protein concentrations were obtained from TSC samples using the Human IGFBP-2 Quantikine ELISA Kit (R&D Systems, Cat. No.: DGB200), according to the manufacturer’s instructions. Quantikine Immunoassay Control Set 1005 for Human IGFBP-2 (R&D Systems, Cat. No.: QC106) was used as a quantitative control. Each sample was tested in duplicate. The optical density of each well was read using a Spark Multimode Microplate Reader (Tecan Trading

AG, Switzerland) at 450 and 570 nm wavelengths, and the concentration of the protein was calculated from the measured absorbance using a standard curve. Additionally, serum samples available from patients without MASLD in the two study groups (IMID and general population) were included as controls.

Statistical analysis

Statistical analyses were performed using SPSS v22.0 (IBM, USA). Group differences in normally distributed values were analyzed by Student’s *t* test or one-way ANOVA, while those of non-normally distributed variables were assessed using the Mann–Whitney *U* test. Categorical comparisons were performed using the chi-square test or Fisher’s exact test, as appropriate. Initial univariate analyses were performed to determine the differences between patients with IMID and the control group, between patients with or without significant liver fibrosis. Raw (unadjusted) and adjusted odds ratios (ORs) with 95% CIs were estimated using stepwise multivariate conditional logistic regression, incorporating variables found to be significant in the univariate analyses, as well as biologically relevant covariates associated with the diagnosis and severity of SLD/MASLD and IMID to test the risk factors for advanced liver fibrosis in our study population. Relative excess risk due to interaction (RERI), was used to assess the additive interaction between IMID and cardiometabolic risk factors. Statistical significance was concluded for two-sided values of *p* <0.05.

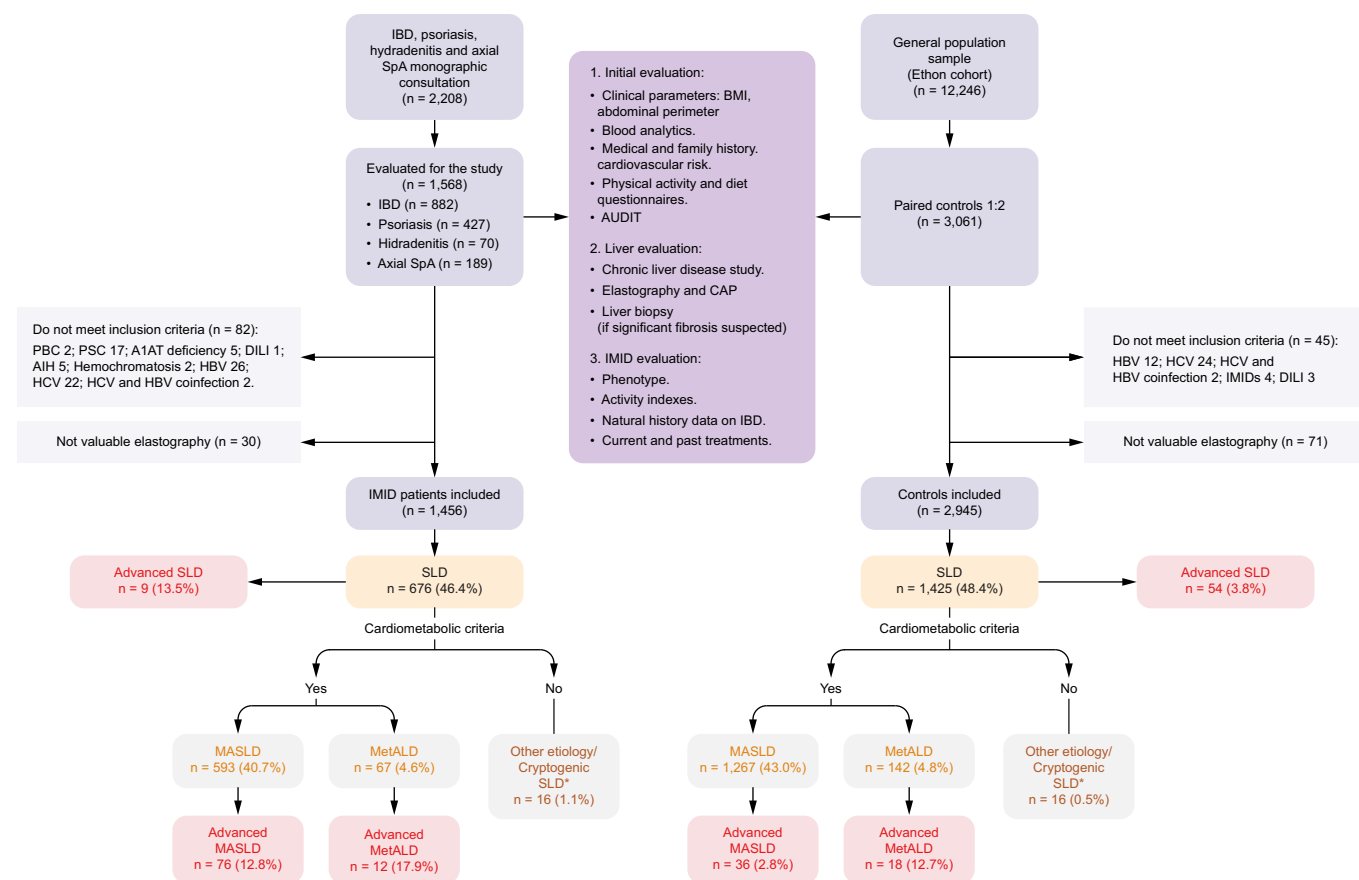


Fig. 1. Study flowchart. A1AT, alpha-1 antitrypsin; AIH, autoimmune hepatitis; ALD, alcohol-associated liver disease; axial SpA, axial spondyloarthritis; IBD, inflammatory bowel disease; PBC, primary biliary cholangitis; PSC, primary sclerosing cholangitis.

Results

Baseline participant characteristics

As illustrated in the study flowchart (Fig. 1), of the 2,208 consecutive patients with IMID assisted at the specific outpatient consultations, 1,566 agreed to participate in the study. A total of 1,456 of the patients met the inclusion criteria and were considered for analysis. A sample of 3,061 controls was drawn from the 12,246 patients in the ETHON cohort. Patients and controls were initially paired at a ratio of 1:2 and evaluated for the study. Finally, 2,945 controls met the inclusion criteria and were enrolled for analysis. The main clinical, anthropometric, and laboratory characteristics of the participants are summarized in Table 1 and Table S1.

Higher prevalence of advanced SLD and advanced MASLD among patients with IMID

We have observed a substantially elevated prevalence of advanced fibrosis concomitant with SLD and MASLD amongst patients with IMID in comparison to controls, notwithstanding the absence of discrepancies in the prevalence of SLD and MASLD between the cohorts (Table 1). The prevalence of

hepatic steatosis attributable to an interplay between cardiometabolic risk factors and alcohol consumption (MetALD) was similarly mirrored between patients with IMID and controls, with no variances in the proportion of advanced fibrosis due to this etiology being detected. We observed a significantly augmented proportion of patients with SLD in the absence of cardiometabolic dysfunction, drug-induced steatosis, or alcohol consumption (cryptogenic SLD) within the IMID group compared to controls. A more granular comparison of SLD characteristics between patients with IMID and controls is delineated in Table S2.

Our analysis extended to the clinical and analytical disparities between patients manifesting advanced fibrosis due to SLD within the IMID cohort and controls (Table 2). Notably, advanced SLD in patients with IMID presents at a markedly younger age and harbors a diminished prevalence of T2D and high-risk alcohol consumption, well documented risk factors for liver fibrosis development in the general population. A more meticulous comparison concerning advanced MASLD in IMID vs. controls can be perused in Table S3. Additionally, we noted a heightened proportion of advanced fibrosis in cryptogenic SLD within the IMID contingent, albeit these differences did not attain statistical significance owing to the paucity of cases. A

Table 1. Baseline clinical and laboratory characteristics of the study population.

	IMID (n = 1,456)	Controls (n = 2,945)	p values
Clinical characteristics			
Age (yr), median (range)	51 (17-83)	51 (18-80)	0.822
Male sex, n (%)	723 (49.7)	1,411 (47.9)	0.276
BMI (kg/m ²), mean (SD)	27.0 ± 5.3	26.9 ± 4.8	0.366
Waist circumference (cm), mean (SD)	94.2 ± 13.3	90.7 ± 14.2	<0.001
T2D, n (%)	117 (8.0)	212 (7.2)	0.320
Hypertension, n (%)	396 (27.2)	596 (20.2)	<0.001
Dyslipidemia*, n (%)	853 (58.6)	1,531 (52.0)	<0.001
Active smoker, n (%)	369/1,379 (26.8)	165/697 (23.7)	0.150
High-risk alcohol intake [#] , n (%)	105 (7.2)	170 (5.8)	0.063
SLD, n (%)	676 (46.4)	1,425 (48.4)	0.221
Advanced SLD, n (%)	91 (13.5)	54 (3.8)	<0.001
MASLD, n (%)	593 (40.7)	1,267 (43.0)	0.424
Advanced MASLD, n (%)	76 (12.8)	36 (2.8)	<0.001
MetALD, n (%)	67 (4.6)	142 (4.8)	0.969
Advanced MetALD, n (%)	12 (17.9)	18 (12.7)	0.314
Cryptogenic [§] SLD, n (%)	16 (1.1)	16 (0.5)	0.036
LSM (kPa), median (range)	5.3 (2.5-59.6)	4.4 (2.5-58.2)	<0.001
CAP (db/m), median (range)	243 (100-400)	246 (100-400)	0.050
Laboratory characteristics, mean (SD)			
Fasting glucose (mg/dl)	82.9 ± 19.1	84.8 ± 21.4	0.003
Triglyceride (mg/dl)	115.9 ± 82.6	140.6 ± 97.2	<0.001
Total cholesterol (mg/dl)	190.7 ± 36.1	201.5 ± 36.6	<0.001
HDL-cholesterol (mg/dl)	56.0 ± 15.9	57.2 ± 15.2	0.017
LDL-cholesterol (mg/dl)	112.8 ± 30.4	116.8 ± 32.6	<0.001
ALT (U/L)	26.0 ± 17.8	26.2 ± 19.7	0.738
Bilirubin (mg/dl)	0.62 ± 0.3	0.55 ± 0.3	<0.001
Albumin (mg/dl)	4.5 ± 0.3	4.4 ± 0.2	<0.001
GFR (ml/min/1.73 m ²)	87.9 ± 7.4	77.6 ± 11.7	<0.001
Hemoglobin (g/dl)	14.1 ± 1.4	13.9 ± 1.3	0.014
Platelet number (10 ³ /μl)	238.4 ± 62.3	228.9 ± 54.0	<0.001
Ferritin (mg/dl)	111.6 ± 141.1	131.2 ± 142.2	<0.001

Differences in characteristics between groups were tested using Student's *t* test in normally distributed and Mann-Whitney *U* test in non-normally distributed variables. Categorical comparisons were performed using chi-square test or Fisher's exact test, as appropriate.

Bold p values indicate statistical significance.

ALT, alanine aminotransferase; CAP, controlled attenuation parameter; IMID, immune-mediated inflammatory diseases; GFR, glomerular filtration rate; HDL, high-density lipoprotein; LDL, low-density lipoprotein; LSM, liver stiffness measurement; MASLD, metabolic dysfunction-associated steatotic liver disease; MetALD, metabolic and high-risk alcohol-associated steatotic liver disease; T2D, type 2 diabetes.

*Dyslipidemia: plasma triglycerides ≥150 mg/dl or HDL-cholesterol lower than 40 mg/dl (M) or 50 mg/dl (F) or lipid-lowering medication.

[#]High-risk alcohol consumption: >20 g/day in women and >30 g/day in men.

[§]Cryptogenic: steatosis in the absence of overt cardiometabolic criteria, drug-induced steatosis or alcohol consumption.

stratified sub-analysis concerning the prevalence of advanced MASLD and metabolic risk factors relative to the type of IMID is exhibited in Fig. S1.

IMID is an independent risk factor for SLD and advanced SLD

Logistic regression analysis showed that a diagnosis of IMID constitutes an independent and paramount risk factor for both SLD (adjusted OR 2.210; 95% CI 1.738-2.810; $p < 0.001$) and advanced SLD (adjusted OR 3.318; 95% CI 2.225-4.947; $p < 0.001$) as illustrated in Fig. 2A,B. Regarding SLD, additional independent risk determinants encompassed age, high-risk alcohol consumption, obesity, dyslipidemia, and waist circumference (WC). Pertaining to advanced SLD, the independent risk factors were identified as high-risk alcohol consumption, T2D, and WC. In light of these findings, we conducted an analysis of the supra-additive effects resulting from the concurrent presentation of IMID with high-risk alcohol consumption, T2D, and a hazardous WC (higher than 94 cm in males or higher than 80 cm in females), employing the calculation of the RERI. Notably, a synergistic effect was discerned in the conjunction of IMID and an increased WC (RERI 2.11; 90% CI 0.02–7.31), depicted in Fig. 3A. However, such synergy was not observed in association with either alcohol or T2D (data not shown).

In an effort to appraise the prevalence of advanced SLD beyond traditional metabolic risk factors, we performed a

stratification of patients with advanced SLD based on the absence of the principal metabolic drivers, specifically T2D, and obesity, as demonstrated in Fig. 3B. Intriguingly, the prevalence of advanced SLD in patients devoid of obesity and/or T2D was significantly elevated in those with IMID compared to controls, with a pronounced augmentation in the absence of T2D (Fig. 3B).

Biological therapy is an independent risk factor for advanced MASLD in the IMID population

Next, to identify the overarching risk factors for advanced SLD within the IMID cohort, our analysis revealed that the requirement for biological therapy emerged as an independent risk factor for advanced SLD, concomitant with an increased WC and the presence of hypertension, as delineated in Fig. 2C. Results from a stratified multivariable logistic regression analysis, tailored to each specific IMID, are comprehensively encapsulated in Table S4. Moreover, our examination discerned no supplementary risk attributable to the utilization of other prevalent medications in IMID treatment known for their potential hepatotoxic association, such as corticosteroids, methotrexate, or immunomodulators, when scrutinizing the collective IMID cohort or individual IMID entities (Table S5). Correspondingly, an analysis focusing on each individual IMID did not unveil any additional risk linked to disease duration or activity (Table S5).

Table 2. Clinical characterization of SLD with advanced fibrosis in patients with IMID and controls.

	Advanced SLD IMID (n = 91)	Advanced SLD controls (n = 54)	p values
Clinical characteristics			
Age (yr), median (range)	54.6 ± 10.63	58.6 ± 9.23	0.020
Male sex, n (%)	53 (58.2)	38 (70.4)	0.099
BMI (kg/m ²), mean (SD)	32.9 ± 6.16	33.9 ± 6.66	0.356
Waist circumference (cm), mean (SD)	110.8 ± 14.99	112.0 ± 14.33	0.648
T2D, n (%)	18 (19.8)	30 (55.6)	<0.001
Hypertension, n (%)	49 (53.8)	29 (53.7)	0.561
Dyslipidemia*, n (%)	66 (72.5)	44 (81.5)	0.316
Active smoker, n (%)	21/78 (26.9)	10/42 (23.8)	0.828
High-risk alcohol [#] , n (%)	12 (13.2)	18 (33.3)	0.006
MASLD, n (%)	76 (83.5)	36 (66.7)	0.025
MetALD, n (%)	12 (13.2)	18 (33.3)	0.006
Cryptogenic, n (%)	3 (3.3)	0 (0)	0.294
CAP (db/m), mean (SD)	325.5 ± 39.83	332.9 ± 46.42	0.316
Laboratory characteristics, mean (SD)			
Fasting glucose (mg/dl)	95.8 ± 31.42	99.1 ± 31.23	0.539
Triglyceride (mg/dl)	167.7 ± 197.15	185.9 ± 100.86	0.532
Total cholesterol (mg/dl)	198.3 ± 49.63	193.2 ± 50.06	0.567
HDL-cholesterol (mg/dl)	53.6 ± 27.86	49.1 ± 14.32	0.284
LDL-cholesterol (mg/dl)	117.8 ± 36.38	109.0 ± 46.21	0.241
ALT (U/L)	44.9 ± 33.69	50.9 ± 32.53	0.300
Bilirubin (mg/dl)	0.6 ± 0.32	0.6 ± 0.33	0.762
Albumin (mg/dl)	4.5 ± 0.27	4.4 ± 0.35	0.342
GFR (ml/min/1.73 m ²)	86.5 ± 10.27	84.3 ± 13.98	0.284
Hemoglobin (g/dl)	14.3 ± 1.51	14.4 ± 1.36	0.825
Platelet (10 ³ /μl)	224.3 ± 73.80	192.9 ± 60.79	0.009
Ferritin (mg/dl)	167.8 ± 245.48	253.6 ± 227.81	0.104

Differences in characteristics between groups were tested using Student's *t* test in normally distributed and Mann-Whitney *U* test in non-normally distributed variables. Categorical comparisons were performed using chi-square test or Fisher's exact test, as appropriate.

Bold p values indicate statistical significance.

ALT, alanine aminotransferase; GFR, glomerular filtration rate; HDL, high-density lipoprotein; IMID, immune-mediated inflammatory diseases; LDL, low-density lipoprotein; LSM, liver stiffness measurement; SLD, steatotic liver disease; T2D, type 2 diabetes.

*Dyslipidemia: plasma triglycerides ≥150 mg/dl or HDL-cholesterol lower than 40 mg/dl (M) or 50 mg/dl (F) or lipid-lowering medication.

[#]High-risk alcohol consumption: >20 g/day in women and >30 g/day in men.

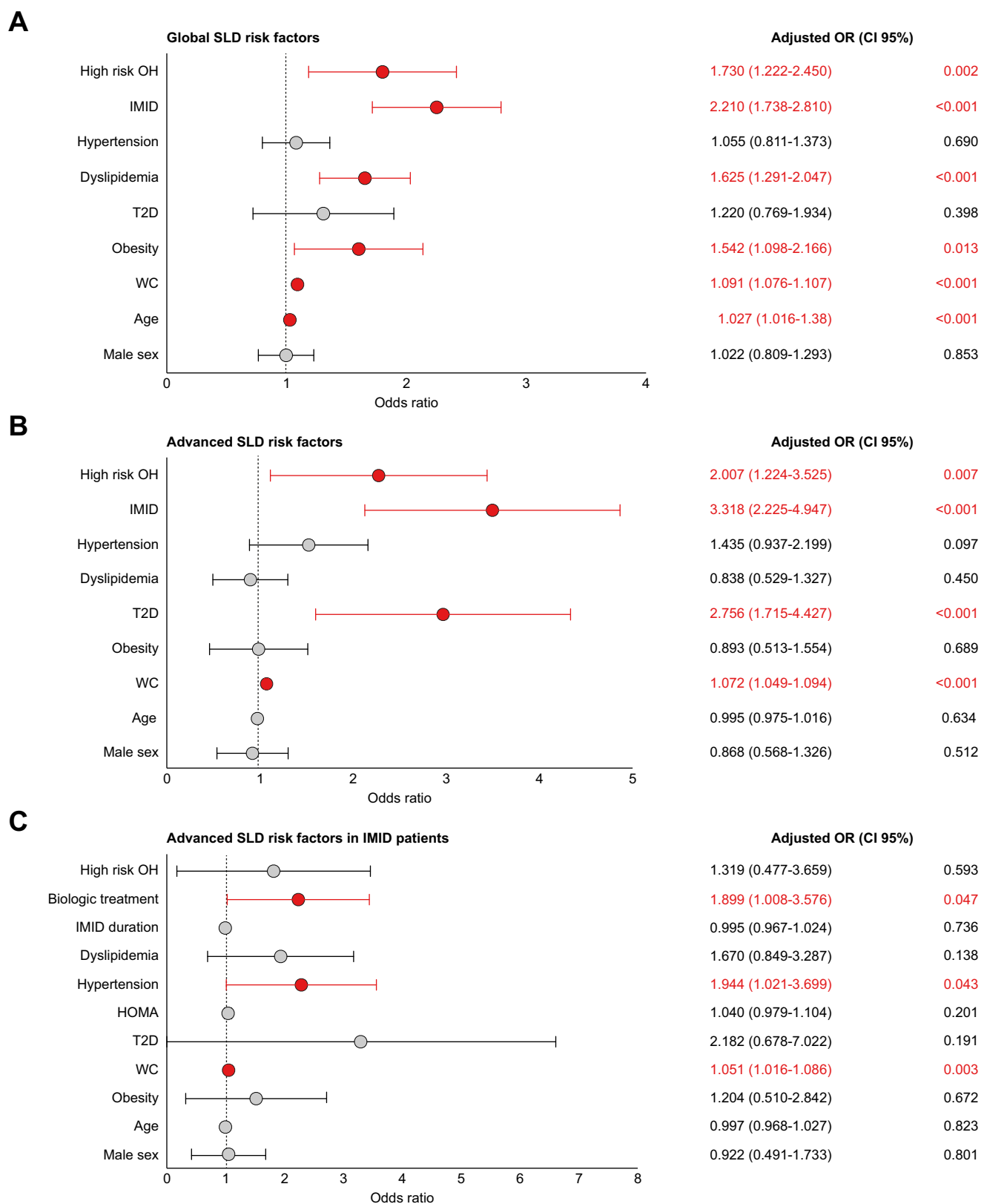


Fig. 2. Logistic regression analysis of SLD and advanced SLD risk factors. (A) Global logistic regression of SLD risk factors, representing adjusted odds ratios with 95% confidence intervals. (B) Global logistic regression of advanced SLD risk factors, representing adjusted odds ratios with 95% confidence intervals. (C) Logistic regression of advanced SLD risk factors in the IMID population, representing adjusted odds ratios with 95% CIs. High-risk OH (alcohol consumption): >20 g/day in women and >30 g/day in men. Stepwise multivariate conditional logistic regression analyses were performed for SLD (A), and advanced SLD (B and C). The models

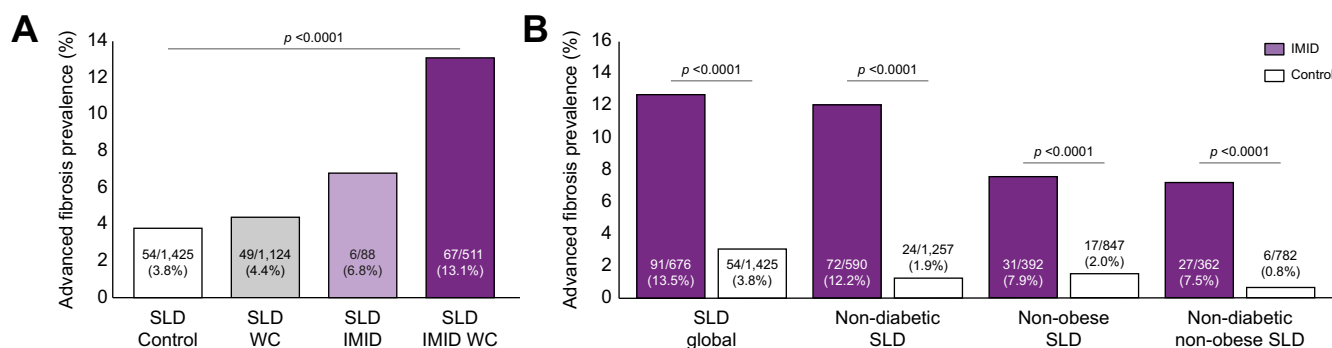


Fig. 3. Advanced SLD prevalence. (A) Supra-additive effect of IMID and hazardous WC on the prevalence of advanced SLD. (B) Advanced fibrosis prevalence attributable to SLD stratified according to the absence of T2D or obesity in IMID and controls. Fisher’s exact tests were performed to obtain *p* values. IMID, immune-mediated inflammatory diseases; SLD, steatotic liver disease; T2D, type 2 diabetes; WC, waist circumference.

Table 3. Comparative analysis of biopsy-proven IMID-MASLD and control-MASLD.

	IMID-MASLD (n = 69)	Control-MASLD (n = 40)	<i>p</i> values
Age (yr), median (range)	54 (27-68)	54 (25-70)	0.782
Male sex, n (%)	38 (55.1)	19 (47.5)	0.446
Hypertension, n (%)	31 (44.9)	27 (67.5)	0.023
T2D, n (%)	20 (29.0)	20 (50.0)	0.028
Obesity, n (%)	44 (63.8)	34 (85.0)	0.018
BMI, mean (±SD)	32.1 ± 6.16	35.7 ± 5.74	0.003
LSM, mean (±SD)	9.1 ± 4.48	9.2 ± 4.2	0.967
Fasting glycaemia, mean (±SD)	98.9 ± 40.13	101.6 ± 20.42	0.010
HbA1c, mean (±SD)	5.7 ± 0.95	5.7 ± 0.63	0.475
Total cholesterol, mean (±SD)	184.3 ± 36.48	170.1 ± 24.94	0.566
HDL-cholesterol, mean (±SD)	49.2 ± 10.23	44.6 ± 9.96	0.001
LDL-cholesterol, mean (±SD)	106.2 ± 33.52	99.6 ± 21.18	0.994
Tryglicerides, mean (±SD)	146.1 ± 57.54	156.85 ± 66.63	0.138
Steatosis, n (%)			0.031
S0	0 (0.0)	0 (0.0)	
S1	39 (56.5)	14 (35.0)	
S2	19 (27.5)	21 (52.5)	
S3	11 (15.9)	5 (12.5)	
Lobular inflammation, n (%)			0.772
0	20 (29.0)	12 (30.0)	
1	32 (46.4)	16 (40.0)	
2	17 (24.6)	12 (30.0)	
3	0 (0.0)	0 (0.0)	
Ballooning, n (%)			0.425
0	16 (23.2)	4 (10.0)	
1	30 (43.5)	24 (60.0)	
2	23 (33.3)	12 (30.0)	
Fibrosis, n (%)			0.316
0	25 (36.2)	11 (27.5)	
1	28 (40.6)	13 (32.5)	
2	5 (7.2)	8 (20.0)	
3	8 (11.6)	6 (15.0)	
4	3 (4.3)	2 (5.0)	

Values in bold denote statistical significance. Differences in characteristics between groups were tested using Student’s *t* test in normally distributed and Mann-Whitney *U* test in non-normally distributed variables. Categorical comparisons were performed using chi-square test or Fisher’s exact test, as appropriate.

IMID, immune-mediated inflammatory diseases; LSM, liver stiffness measurement; MASLD, metabolic dysfunction-associated steatotic liver disease; T2D, type 2 diabetes.

Distinctive clinical and histological profiles in a cohort of biopsy-proven MASLD in IMID and controls

To identify the specific molecular mechanisms potentially implicated in the pathobiology of SLD in patients with IMID and controls, we collected a TSC of 109 histologically characterized

cases (69 IMID and 40 control). All cases included in both the IMID cohort, and the controls meet the clinical diagnostic criteria for MASLD; henceforth, we will refer to them as IMID-MASLD and control-MASLD. None of the cases selected in the IMID cohort were undergoing treatment associated with

were adjusted for all the variables shown in the table. Statistically significant variables are indicated in red. IMID, immune-mediated inflammatory diseases; OR, odds ratio; SLD, steatotic liver disease; T2D, type 2 diabetes; WC, waist circumference.

hepatotoxicity (such as methotrexate or corticosteroids), although 33 of them (47.8%) had received one of these treatments in the past. Additionally, 15 patients were receiving monoclonal antibody therapy at the time of biopsy (21.7%). Liver biopsies were obtained when significant liver fibrosis was suspected according to LSM in both groups of patients. According to the study protocol, IMID-MASLD biopsies were paired with control-MASLD cases by age and grade of liver fibrosis to enable a comparison between the clinical and histological profiles of IMID- and control-MASLD with equivalent disease severity. The main components of metabolic syndrome (T2D, obesity, and hypertension) were significantly underrepresented in the IMID-MASLD group compared to the control-MASLD group (Table 3). This observation was further supported by the distinctively better glucose and lipid metabolism profiles in the IMID-MASLD cases. In terms of histology, for an equivalent degree of fibrosis, IMID-MASLD biopsies displayed a significantly lower grade of steatosis, with similar levels of lobular inflammation and hepatocellular ballooning.

Transcriptomic analysis shows alternative mechanisms driving IMID-MASLD

The abovementioned clinical and histological data suggest that independent mechanisms/molecules might drive the

pathogenesis of IMID-vs. control-MASLD. Thus, we performed a comparative mRNA-seq transcriptome analysis in TSC using a statistical model adjusted for BMI, sex, and fibrosis severity. Under these conditions, we detected 87 significant genes that were differentially expressed ($p_{adj} < 0.05$, Table S6). In this context, a heatmap showing the expression levels of the differentially expressed genes and clustering among cases from each group is shown in (Fig. 4A). More specifically, whereas genes such as *IGFBP2*, *LRCOL1* and *PLHDA1* were upregulated in IMID-MASLD, others such as dopamine receptor D1 (*DRD1*), perilipin 1 (*PLIN1*) and the metallothioneins *MT1M*, *MT1G* and *MT1F* were downregulated (Fig. 4B). These genes are widely expressed in the liver (mostly in hepatocytes) and can participate in the development and progression of cancers, such as renal cell carcinoma (*i.e.*, *IGFBP2* and metallothioneins *MT1H*, *MT1F*, or *MT1G*) and hepatocellular carcinoma (*i.e.*, *GPX2*, *LRCOL1* and *PLEKHA4*)^{19,20} (proteinatlas.org) (Fig. 4B). Since *IGFBP2* (insulin-like growth factor binding protein 2) was the top hit expressed in IMID-MASLD liver biopsies, we sought to analyze its correlation with serum protein levels. Our data confirmed significantly higher levels of *IGFBP2* in serum from patients with IMID-MASLD (Fig. S2). Similar *IGFBP2* serum expression levels were found between IMID-MASLD, IMID and control patients without MASLD.

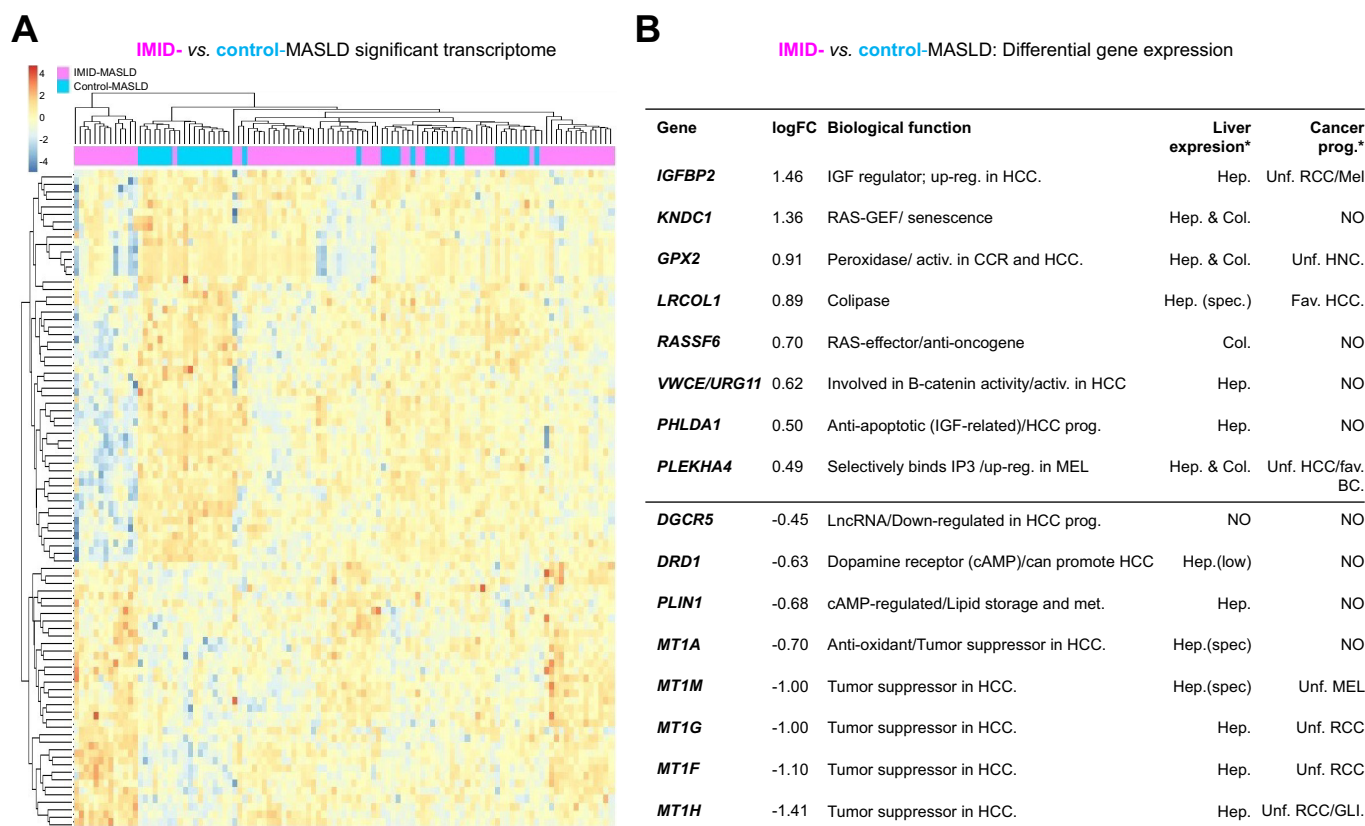


Fig. 4. Differential gene expression in IMID-MASLD vs. control-MASLD. (A) Heatmap showing mRNA expression values and clustering of the 87 differentially expressed genes (row-scaled logCPM values) in the TSC cohort of MASLD cases ($n = 109$). Pink and blue boxes correspond to IMID-MASLD and control-MASLD cases, respectively. (B) Representative selection of upregulated ($\logFC > 0.40$) and downregulated genes ($\logFC < -0.40$), ($p_{adj} < 0.05$) from those shown in (A). Activ, activated; Col, cholangiocyte; Fav, favorable; GLI, glioma; HCC, hepatocellular carcinoma; Hep, hepatocytes; IMID, immune-mediated inflammatory diseases; LogFC, log fold-change; MASLD, metabolic dysfunction-associated steatotic liver disease; MEL, melanoma; Prog, progression; RCC, renal cell carcinoma; TSC, translational study cohort; Unf, unfavorable.

To better understand the cellular functions and mechanisms associated with the differentially expressed genes, we performed a gene set-enrichment analysis that detected the most relevant gene sets differentially enriched in IMID-MASLD cases (Table S7). Among the latter, positively enriched gene sets were detected with their associated activities related to the control of DNA synthesis and the cell cycle, RHO-GTPase signaling towards the actin cytoskeleton and oncogene-related signaling involving RAS-MAPK and proinflammatory IL6 (Fig. 5). In contrast, negatively enriched gene sets in IMID-MASLD were associated with peroxisomal activity, response to metal ions, mitochondrial and lipid metabolism, and dopamine signaling.

In addition, the transcriptomic analysis of IMID-vs. control-MASLD stratified according to the presence of absent/mild (F0-F1) vs. significant/advanced liver fibrosis (\geq F2) showed

increased mRNA expression of *IGFBP2*, *PLEKHA4* and *FARP1* in patients with IMID-MASLD and mild fibrosis (Fig. S3A). *IGFBP2* serum levels correlated with the transcriptomic data (Fig. S3B). Patients with IMID-MASLD and significant or advanced fibrosis (\geq F2) displayed upregulated expression of *LRCOL1* (colipase), *CCL19* (an inflammatory cytokine) and *cMYC* (*MYC* oncogene) and reduced expression of *DRD1* and metallothioneins (Table S8).

Discussion

Despite the previously described increased prevalence of MASLD associated with several IMIDs, clinical and molecular characterization of MASLD developing on an IMID background, as a condition distinct from classic metabolic risk factors, has

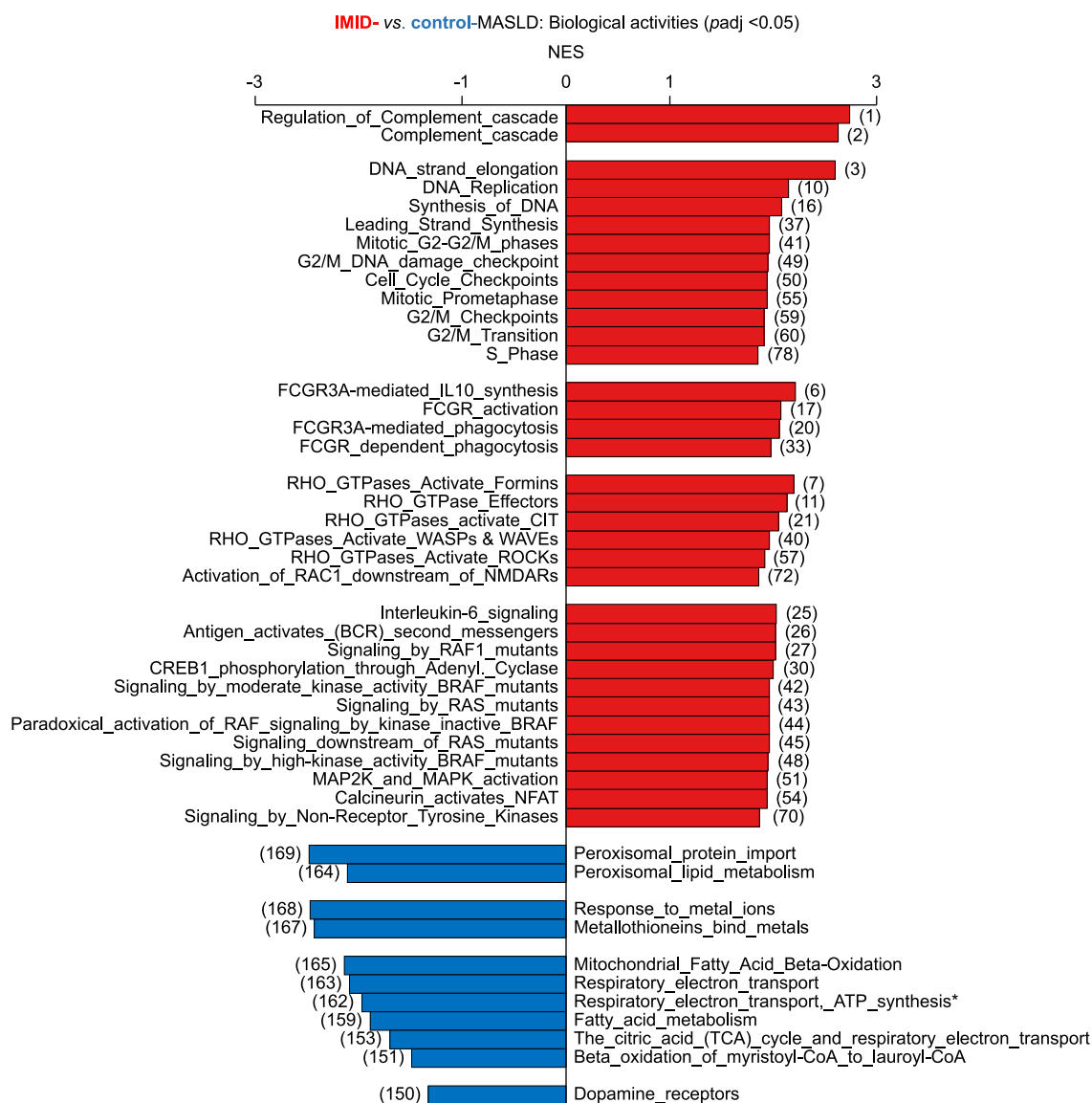


Fig. 5. Differential gene set-enrichment analysis in IMID-MASLD vs. control-MASLD. A selection of positively (red) and negatively (blue) differential gene set-enrichment (stratified by biological activities) between IMID- and control-MASLD patients, (*padj* < 0.05). Numbers in the scale show NESs. Numbers in brackets indicate pathway position in the full report (supp. Table 8). Pathway positions range 1-149 for positive NES and 150-169 for negative NES. IMID, immune-mediated inflammatory diseases; MASLD, metabolic dysfunction-associated steatotic liver disease; NESs, normalized enrichment scores.

not been conducted. From a clinical perspective, we have discerned an elevated prevalence of advanced SLD and advanced MASLD in patients with IMID, irrespective of classic metabolic risk factors. We deem this observation to be of paramount significance, as it may engender heightened vigilance for advanced liver disease risk across various medical disciplines overseeing patients with IMID. This augmented risk may be attributable to the interplay between chronic inflammation, inherent to IMIDs, and cardiometabolic disturbances. This was exemplified in our multivariate analysis of advanced SLD risk factors in patients with IMID (Fig. 2C), wherein we observed an amalgamation of classic metabolic risk factors, such as augmented waist circumference or hypertension, concomitant with factors associated with IMID severity, such as the need for biological treatment – a surrogate marker of the IMID inflammatory burden. Furthermore, supporting the potential supra-additive magnitude of the interaction between IMID diagnosis and cardiometabolic criteria, we have noted a remarkably high prevalence of advanced SLD in patients with a concurrent diagnosis of IMID and a hazardous increase in WC, highlighting the synergistic effect of the coexistence of both conditions.

In our cohort, patients with advanced SLD or advanced MASLD and IMID were significantly younger and exhibited a markedly lower prevalence of T2D or hazardous alcohol intake, in the case of SLD, compared to controls. In addition, the prevalence of advanced SLD was substantially higher among non-obese, non-diabetic, and non-obese or diabetic IMID cases than in controls. These findings, in conjunction with the elevated prevalence of cryptogenic SLD among IMID cases, suggest an independent and specific etiology beyond classic metabolic risk factors, accounting for a more progressive form of SLD in these patients. The natural history of MASLD in lean individuals remains elusive. Consonant with our findings, recent research has demonstrated that, despite a more favorable metabolic profile, lean individuals with MASLD face similar risks of disease progression to MASH and cirrhosis.^{21,22} Moreover, although only a limited corpus of studies has explored the distinctive mortality rates and clinical outcomes between lean and non-lean patients with MASLD, the extant data suggest that lean individuals with MASLD are exposed to comparable, if not heightened, risks of progressive liver disease, cancer, and all-cause mortality.²¹ Our study furnishes a functional elucidation for the IMID paradigm.

Firstly, in relation to cancer risk, we note that functionally, IMID-MASLD cases within the TSC cohort exhibit upregulated expression of gene sets directly implicated in cell proliferation, oncogenic, and inflammatory signaling pathways, such as RAS-MAPK signaling and the proinflammatory cytokine IL6. Conversely, these cases demonstrate suppressed expression of genes associated with peroxisomal activity, mitochondrial and lipid metabolism, metallothioneins, and dopamine signaling. Notably, IMID-MASLD-upregulated genes are significantly linked to the biology of various human cancers, including *GPX2* and *URG11* in HCC,^{19,23} *PLEKHA4* in melanoma²⁴, and *IGFBP2* in renal cell carcinoma.²⁵ Furthermore, diminished metallothionein expression, as observed in IMID-MASLD cases, is likewise correlated with the development of numerous human cancers, including HCC.²⁶ Mechanistically, these genes can participate in well-known oncogenic signaling

pathways such as *URG11*, *PLEKHA4*, *GPX2* and metallothioneins in the WNT-beta catenin pathway, which is highly implicated in the development of liver adenomas and HCC.^{23,24,26–29} Additionally, certain IMID-MASLD-upregulated genes, such as *RASSF6*, which functions as an anti-oncogene, may play a role in curtailing cellular cytotoxicity/transformation in this biological milieu.³⁰ These findings disclose a pathophysiological context consistent with a protumoral condition conducive to the emergence of an expedited and more progressive form of SLD/MASLD in patients with IMID, even in the absence of obesity. Intriguingly, notwithstanding the deleterious impact of obesity on overall health, recent studies have elucidated that the risk of cancer escalates in MASLD, independently of obesity.³¹

Secondly, regarding the risk of progressive liver disease, it is noteworthy that T2D, a well-documented driver of fibrosis in MASLD, is less prevalent among patients with advanced SLD/MASLD and IMID compared to controls. Remarkably, about 3/10 patients with advanced fibrosis within the IMID population (27/91; 29.7%) were non-obese and non-diabetic, a proportion significantly exceeding that observed in control-SLD (6/54; 11.1%) ($p = 0.013$). Additionally, patients with advanced MASLD in the IMID cohort were significantly younger (see Table 2 and Table S3). As previously mentioned, these data imply an accelerated and more severe form of MASLD in the context of IMIDs. In this context, the expression of *SERPINA1* (*PI*) was upregulated in IMID-MASLD cases (see Table S6). Since it is well established that accumulative protein variants of *SERPINA1* (*PIZ*) in hepatocytes correlate with enhanced inflammatory activity and fibrosis stage in patients with concurrent liver disease,³² it is plausible that its enhanced expression may contribute to the accelerated progression of IMID-MASLD described in this study. Patients with a concomitant diagnosis of alpha-1 antitrypsin deficiency were excluded from the analysis. An additional intriguing mechanism within IMID-MASLD involves compromised dopamine signaling through reduced *DRD1* and *PLIN1* expression. Upon activation, *DRD1* signals via cAMP and promotes phosphorylation of *PLIN1*, which is involved in lipid droplet formation and fatty acid lipolysis.³³ In agreement with the antagonistic role of *DRD1* in IMID-MASLD, it has been shown that *DRD1* activation prevents fibrosis in mice via *YAP/TAZ* activity impairment.³⁴ While the precise contribution of these findings remains to be elucidated, they might incite MASLD development through pathways alternative to classic metabolic factors.

In a concurrent transcriptome analysis stratified according to the degree of liver fibrosis, substantial *IGFBP2* overexpression was observed in IMID-MASLD cases at the early stages of the disease (F0–F1), which can also indicate a distinctive yet accelerated liver disease process. Moreover, cases with F ≥ 2 exhibited overexpression of the cMYC oncogene and *CCL19*, a proinflammatory cytokine. While cMYC serves as a key transcriptional regulator of metabolism and cancer, particularly implicated in hepatocyte proliferation, liver regeneration, and fibrogenesis,^{35,36} *CCL19* functions as a T-cell chemoattractant via *CCR7*, also highly involved in HCC progression.^{37,38} These results support the idea of cell transforming mechanisms participating in the more aggressive IMID-MASLD, as judged by the higher prevalence of advanced liver fibrosis in an IMID context.

The principal drivers of MASLD in the absence of overweight/obesity and T2D remain elusive. Potential factors include genetic, environmental, endocrine, or inflammatory agents that can interact and modulate susceptibility to MASLD without excess body adiposity.⁵ Our transcriptomic analysis revealed a distinctive molecular signature that supports a “nonmetabolic” background in IMID-MASLD. In this sense, the most highly upregulated gene in IMID-MASLD, *IGFBP2*, can exemplify this “nonmetabolic” signature. Specifically, *IGFBP2*, the most prominently upregulated gene in IMID-MASLD, epitomizes this “nonmetabolic” signature. *IGFBP2* mRNA expression was significantly upregulated in IMID-MASLD cases, accounting for notably lower serum insulin levels compared with classic MASLD (see Table S3). We further corroborated this expression at the protein level in serum samples. Functionally, *IGFBP2* has been illustrated to bind and modulate the activities of IGF1 and IGFII, either augmenting or diminishing their effects.³⁹ *IGFBP2* serves as a biomarker for metabolic syndrome; in states of obesity, its circulating levels are diminished, and its low concentrations are strongly correlated with T2D and metabolic syndrome.⁴⁰ Studies involving transgenic mice overexpressing human *IGFBP2* have showcased its protective role in glucose resistance, which is both age- and diet-dependent.⁴¹ Additionally, *IGFBP2* is implicated in pro-tumoral activities and the advancement of various human cancers, including ovarian, breast, prostate, renal cell, and hepatocellular carcinoma.^{25,39,42} Considering the inverse association between *IGFBP2* expression and the incidence of classic MASLD,⁴³ our findings advocate for the activation of alternative mechanisms by chronic inflammation, diverging from classic metabolic disorders, in the development of liver disease.

Our study is not without limitations. Firstly, the presumption of advanced liver fibrosis was predicated on TE results. Despite liver biopsies being obtained from patients with suspected liver fibrosis, our study design precluded an analysis of TE’s diagnostic efficacy for advanced MASLD within the IMID cohort.

However, the assumption of liver fibrosis was established based on TE in both the case and control groups, facilitating a comparative analysis between the two cohorts. Secondly, the IMID cohort comprised four distinct conditions, each with varying metabolic profiles (see Fig. S1). Despite this heterogeneity, the data on the elevated risk for advanced SLD were consistent across all four conditions, underscoring the pivotal role of non-invasive risk assessment for advanced fibrosis in patients with IMID. Lastly, the patients with IMID included in our study received various treatments pertinent to their IMIDs, which may have potentially influenced the transcriptomic outcomes. Nonetheless, we did not identify any statistical linkage between the use of potentially steatogenic medications and the prevalence of advanced SLD. The prospect of conducting an analysis on a treatment-naïve IMID patient cohort who have developed complications due to their chronic inflammatory state is highly improbable, leading us to posit that our molecular data, whether influenced by pharmacological mechanisms or not, represent a progression in the comprehension of the pathogenic mechanisms behind advanced SLD arising in the milieu of immune-mediated diseases.

In summary, advanced SLD and MASLD exhibit a disproportionately high prevalence in IMID populations, independent of metabolic dysfunction and high-risk alcohol consumption. Supporting this, we provide a functional explanation differentiating between IMID- and control-MASLD and demonstrate that IMIDs manifest a distinctive gene expression signature involved in cellular processes consistent with a pro-tumoral liver condition. This paves the way to an accelerated and aggressive form of MASLD that develops autonomously from classical metabolic pathways. Our revelations constitute a significant stride in the understanding of the pathophysiology underlying the heterogeneity of MASLD/SLD beyond metabolic syndrome. These insights may serve as a foundation for future research into targeted therapies tailored for IMID-MASLD patients.

Affiliations

¹Clinical and Translational Research in Digestive Diseases. Valdecilla Research Institute (IDIVAL). Santander, Spain; ²Gastroenterology and Hepatology Department. University Hospital Marqués de Valdecilla. Santander, Spain; ³Pathological Anatomy Service. University Hospital Marqués de Valdecilla. Santander, Spain; ⁴Division of Rheumatology. University Hospital Marqués de Valdecilla. Santander, Spain; ⁵Dermatology Department. University Hospital Marqués de Valdecilla. Santander, Spain; ⁶CNAG-CRG, Centre for Genomic Regulation (CRG), Barcelona Institute of Science and Technology (BIST); Universitat Pompeu Fabra (UPF), Barcelona, Spain; ⁷Molecular Biology Department-Transkin Research Group. Universidad de Cantabria. Santander (Spain)

Abbreviations

CAP, controlled attenuation parameter; IBD, inflammatory bowel disease; IMID, immune-mediated inflammatory diseases; LSM, liver stiffness measurement; MASH, metabolic dysfunction-associated steatohepatitis; MASLD, metabolic dysfunction-associated steatotic liver disease; MetALD, metabolic and high-risk alcohol-associated steatotic liver disease; NES, normalized enrichment score; OR, odds ratio; RERI, relative excess risk due to interaction; SLD, steatotic liver disease; TE, transient elastography; TSC, translational study cohort; WC, waist circumference.

Financial acknowledgement

This work was fully supported by grants from the Spanish Instituto de Salud Carlos III (ISCIII-FEDER). Grant numbers: PI18/01304, PI20/01279, and PI19/00204.

Conflict of interest

María Teresa Arias-Loste reports research support from Novo Nordisk, travel grants from Gilead Sciences, and is a consultant for Novo Nordisk and MSD (none of them related to the submitted work). Javier Crespo reports grants and

research support from Gilead Sciences, Echosens, AbbVie, MSD, Shionogi, and Intercept Pharmaceuticals (none of them related to the submitted work). Is a speaker for Gilead Sciences and AbbVie. The rest of the authors report no relevant conflicts of interest or disclosures relevant to this manuscript.

Please refer to the accompanying ICMJE disclosure forms for further details.

Authors' contributions

Conception and design: Vaque, Arias-Loste, Crespo. Acquisition of clinical and laboratory data: García-Nieto, Rodríguez-Duque, Rivas-Rivas, Rueda-Gotor, Iruzubieta, Castro, García-García. Data processing: Rasines, Alvarez-Cancelo, García-Nieto, García-Blanco. Diagnostic procedures: Fortea, Puente, Rivero, Blanco, Armesto, González-López, Cagigal. Experimental procedures: García-Blanco, Alvarez-Cancelo, García-Nieto, Vaque. Analysis and interpretation of data: Esteve-Codina, Gut, García-Nieto, Rodríguez-Duque, Vaqué, Arias-Loste, Crespo. Drafting of the manuscript: Vaqué, García-Nieto, Rodríguez-Duque, Arias-Loste, Crespo. Critical revision of the manuscript for intellectual content: Puente, Fortea, Iruzubieta, Blanco, Rivero, Vaqué, Arias-Loste, Crespo. Statistical analysis: Gut, Esteve-Codina, Rodríguez-Duque, Arias-Loste. Obtaining funding: Vaque, Arias-Loste, Crespo. Supervision: Arias-Loste, Crespo.

Data availability statement

Data from the database that support the findings of this study are available from the corresponding author upon reasonable request. Transcriptomic data supporting the findings of this study are publicly available in the Gene Expression Omnibus repository (GEO; NCB) (Identifier: GSE268273) and can be accessed at:

=[https://urldefense.com/v3/_https://www.ncbi.nlm.nih.gov/geo/query/acc.cgi?acc=GSE268273_!!D9dNQwwGXtA!Wsv5jQl2zeVihDnDKahMUP9jpKknr9W4SyL0moTm0G7RTakmxlad5X0dEdofZRTroSElff_oESsGIPY6LF7mdQ\\$](https://urldefense.com/v3/_https://www.ncbi.nlm.nih.gov/geo/query/acc.cgi?acc=GSE268273_!!D9dNQwwGXtA!Wsv5jQl2zeVihDnDKahMUP9jpKknr9W4SyL0moTm0G7RTakmxlad5X0dEdofZRTroSElff_oESsGIPY6LF7mdQ$).

Supplementary data

Supplementary data to this article can be found online at <https://doi.org/10.1016/j.jhepr.2024.101167>.

References

Author names in bold designate shared co-first authorship

- [1] Riazi K, Azhari H, Charette JH, et al. The prevalence and incidence of NAFLD worldwide: a systematic review and meta-analysis. *Lancet Gastroenterol Hepatol* 2022;7:851–861. [https://doi.org/10.1016/S2468-1253\(22\)00165-0](https://doi.org/10.1016/S2468-1253(22)00165-0).
- [2] Younossi Z, Anstee QM, Marietti M, et al. Global burden of NAFLD and NASH: trends, predictions, risk factors and prevention. *Nat Rev Gastroenterol Hepatol* 2017;15(1):11–20. <https://doi.org/10.1038/nrgastro.2017.109>.
- [3] Younossi ZM, Golabi P, De Avila L, et al. The global epidemiology of NAFLD and NASH in patients with type 2 diabetes: a systematic review and meta-analysis. *JOURNAL OF HEPATOLOGY* the global epidemiology of NAFLD and NASH in patients with type 2 diabetes: a systematic review and meta-analysis. *J Hepatol* 2019;71:793–801. <https://doi.org/10.1016/j.jhep.2019.06.021>.
- [4] Matteoni CA, Younossi ZM, Gramlich T, et al. Nonalcoholic fatty liver disease: a spectrum of clinical and pathological severity. *Gastroenterology* 1999;116:1413–1419.
- [5] DiStefano JK, Gerhard GS. NAFLD in normal weight individuals. *Diabetol Metab Syndr* 2022;14:1–18. <https://doi.org/10.1186/S13098-022-00814-Z/TABLES/3>.
- [6] Rodriguez-Duque JC, Calleja JL, Iruzubieta P, et al. Increased risk of MAFLD and liver fibrosis in inflammatory bowel disease independent of classic metabolic risk factors. *Clin Gastroenterol Hepatol* 2023;21:406–414.e7. <https://doi.org/10.1016/j.cgh.2022.01.039>.
- [7] Duran-Vian C, Arias-Loste MT, Hernandez JL, et al. High prevalence of non-alcoholic fatty liver disease among hidradenitis suppurativa patients independent of classic metabolic risk factors. *J Eur Acad Dermatol Venereol* 2019. <https://doi.org/10.1111/jdv.15764>.
- [8] El-Gabalawy H, Guenther LC, Bernstein CN. Epidemiology of immune-mediated inflammatory diseases: incidence, prevalence, natural history, and comorbidities. *J Rheumatol* 2010;37:2–10. <https://doi.org/10.3899/jrheum.091461>.
- [9] Agca R, Smulders Y, Nurmohamed M. Cardiovascular disease risk in immune-mediated inflammatory diseases: recommendations for clinical practice. *Heart* 2022;108:73–79. <https://doi.org/10.1136/HEARTJNL-2019-316378>.
- [10] Crespo J, Cuadrado A, Perelló C, et al. Epidemiology of hepatitis C virus infection in a country with universal access to direct-acting antiviral agents: data for designing a cost-effective elimination policy in Spain. *J Viral Hepat* 2020;27:360–370. <https://doi.org/10.1111/jvh.13238>.
- [11] Chalasani N, Younossi Z, Lavine JE, et al. The diagnosis and management of nonalcoholic fatty liver disease: practice guidance from the American Association for the Study of Liver Diseases. *Hepatology* 2018;67:328–357. <https://doi.org/10.1002/hep.29367>.
- [12] Karlas T, Petroff D, Sasso M, et al. Individual patient data meta-analysis of controlled attenuation parameter (CAP) technology for assessing steatosis. *J Hepatol* 2016. <https://doi.org/10.1016/j.jhep.2016.12.022>.
- [13] Rinella ME, Lazarus JV, Ratzliff V, et al. A multisociety Delphi consensus statement on new fatty liver disease nomenclature. *J Hepatol* 2023;79:1542–1556. <https://doi.org/10.1016/j.jhep.2023.06.003>.
- [14] Eddowes PJ, Sasso M, Allison M, et al. Accuracy of FibroScan controlled attenuation parameter and liver stiffness measurement in assessing steatosis and fibrosis in patients with nonalcoholic fatty liver disease. *Gastroenterology* 2019;156:1717–1730. <https://doi.org/10.1053/j.gastro.2019.01.042>.
- [15] Dobin A, Davis CA, Schlesinger F, et al. STAR: ultrafast universal RNA-seq aligner. *Bioinformatics* 2013;29:15–21. <https://doi.org/10.1093/BIOINFORMATICS/BTS635>.
- [16] Li B, Dewey CN. RSEM: accurate transcript quantification from RNA-Seq data with or without a reference genome. *BMC Bioinformatics* 2011;12:1–16. <https://doi.org/10.1186/1471-2105-12-323/TABLES/6>.
- [17] Law CW, Chen Y, Shi W, et al. Voom: precision weights unlock linear model analysis tools for RNA-seq read counts. *Genome Biol* 2014;15:1–17. <https://doi.org/10.1186/GB-2014-15-2-R29/FIGURES/11>.
- [18] Korotkevich G, Sukhov V, Budin N, et al. Fast gene set enrichment analysis. *BioRxiv* 2021:060012. <https://doi.org/10.1101/060012>.
- [19] Liu T, Kan XF, Ma C, et al. GPX2 overexpression indicates poor prognosis in patients with hepatocellular carcinoma. *Tumour Biol : J Int Soc Oncodevelopmental Biol Med* 2017;39. <https://doi.org/10.1157/1010428317700410>.
- [20] Uhlén M, Fagerberg L, Hallström BM, et al. Proteomics. Tissue-based map of the human proteome. *Science (New York, NY)* 2015;347. <https://doi.org/10.1126/SCIENCE.1260419>.
- [21] Ahmed OT, Gidener T, Mara KC, et al. Natural history of nonalcoholic fatty liver disease with normal body mass index: a population-based study. *Clin Gastroenterol Hepatol : Official Clin Pract J Am Gastroenterological Assoc* 2022;20:1374–1381.e6. <https://doi.org/10.1016/J.CGH.2021.07.016>.
- [22] Denkmayr L, Feldman A, Stechemesser L, et al. Liver patients with non-alcoholic fatty liver disease have a severe histological phenotype similar to obese patients. *J Clin Med* 2018;7. <https://doi.org/10.3390/JCM7120562>.
- [23] Fan R, Li X, Du W, et al. Adenoviral-mediated RNA interference targeting URG11 inhibits growth of human hepatocellular carcinoma. *Int J Cancer* 2011;128:2980–2993. <https://doi.org/10.1002/IJC.25624>.
- [24] Shah AS, Cao X, White AC, et al. PLEKHA4 promotes Wnt/ β -catenin signaling-mediated G1-S transition and proliferation in Melanoma. *Cancer Res* 2021;81:2029–2043. <https://doi.org/10.1158/0008-5472.CAN-20-2584/654307/AM/PLEKHA4-PROMOTES-WNT-BETA-CATENIN-SIGNALING>.
- [25] Katayama H, Tamai K, Shibuya R, et al. Long non-coding RNA HOTAIR promotes cell migration by upregulating insulin growth factor-binding protein 2 in renal cell carcinoma. *Scientific Rep* 2017;7. <https://doi.org/10.1038/S41598-017-12191-Z>.
- [26] Si M, Lang J. The roles of metallothioneins in carcinogenesis. *J Hematol Oncol* 2018;11. <https://doi.org/10.1186/S13045-018-0645-X>.
- [27] Tian Y, Mok MTS, Yang P, et al. Epigenetic activation of wnt/ β -catenin signaling in NAFLD-associated hepatocarcinogenesis. *Cancers* 2016;8. <https://doi.org/10.3390/CANCERS8080076>.
- [28] Zheng Y, Jiang L, Hu Y, et al. Metallothionein 1H (MT1H) functions as a tumor suppressor in hepatocellular carcinoma through regulating Wnt/ β -catenin signaling pathway. *BMC Cancer* 2017;17:161. <https://doi.org/10.1186/S12885-017-3139-2>.
- [29] Esworthy RS, Doroshov JH, Chu FF. The beginning of GPX2 and 30 years later. *Free Radic Biol Med* 2022;188:419–433. <https://doi.org/10.1016/J.FREERADBIOMED.2022.06.232>.
- [30] Zhu N, Si M, Yang N, et al. Overexpression of RAS-association domain family 6 (RASSF6) inhibits proliferation and tumorigenesis in hepatocellular carcinoma cells. *Oncol Res* 2017;25:1001–1008. <https://doi.org/10.3727/096504016X14796039599926>.
- [31] Allen AM, Hicks SB, Mara KC, et al. The risk of incident extrahepatic cancers is higher in non-alcoholic fatty liver disease than obesity - a longitudinal cohort study. *J Hepatol* 2019;71:1229–1236. <https://doi.org/10.1016/J.JHEP.2019.08.018>.
- [32] Fischer HP, Ortiz-Pallardó ME, Ko Y, et al. Chronic liver disease in heterozygous alpha1-antitrypsin deficiency. *PiZ. J Hepatol* 2000;33:883–892. [https://doi.org/10.1016/S0168-8278\(00\)80119-1](https://doi.org/10.1016/S0168-8278(00)80119-1).
- [33] Ramms DJ, Raimondi F, Arang N, et al. G α s-protein kinase A (PKA) pathway signalopathies: the emerging genetic landscape and therapeutic potential of human diseases driven by aberrant G α s-PKA signaling. *Pharmacol Rev* 2021;73:1326–1368. <https://doi.org/10.1124/PHARMREV.120.000269>.
- [34] Haak AJ, Kostallari E, Sicard D, et al. Selective YAP/TAZ inhibition in fibroblasts via dopamine receptor D1 agonism reverses fibrosis. *Sci Translational Med* 2019;11. <https://doi.org/10.1126/SCITRANSLMED.AAU6296>.
- [35] Zheng K, Cubero FJ, Nevzorova YA. c-MYC—making liver sick: role of c-MYC in hepatic cell function, homeostasis and disease. *Genes* 2017;8:2–20. <https://doi.org/10.3390/GENES8040123>.
- [36] Nevzorova YA, Hu W, Cubero FJ, et al. Overexpression of c-myc in hepatocytes promotes activation of hepatic stellate cells and facilitates the onset of liver fibrosis. *Biochim Biophys Acta* 2013;1832:1765–1775. <https://doi.org/10.1016/J.BBADIS.2013.06.001>.

- [37] Yang L, Chang Y, Cao P. CCR7 preservation via histone deacetylase inhibition promotes epithelial-mesenchymal transition of hepatocellular carcinoma cells. *Exp Cell Res* 2018;371:231–237. <https://doi.org/10.1016/J.YEXCR.2018.08.015>.
- [38] Shi JY, Yang LX, Wang ZC, et al. CC chemokine receptor-like 1 functions as a tumour suppressor by impairing CCR7-related chemotaxis in hepatocellular carcinoma. *J Pathol* 2015;235:546–558. <https://doi.org/10.1002/PATH.4450>.
- [39] Hoeflich A, Russo VC. Physiology and pathophysiology of IGFBP-1 and IGFBP-2 - consensus and dissent on metabolic control and malignant potential. *Best Pract Res Clin Endocrinol Metab* 2015;29:685–700. <https://doi.org/10.1016/J.BEEM.2015.07.002>.
- [40] Heald AH, Kaushal K, Siddals KW, et al. Insulin-like growth factor binding protein-2 (IGFBP-2) is a marker for the metabolic syndrome. *Exp Clin Endocrinol Diabetes* 2006;114:371–376. <https://doi.org/10.1055/S-2006-924320/ID/28>.
- [41] Wheatcroft SB, Kearney MT, Shah AM, et al. IGF-binding protein-2 protects against the development of obesity and insulin resistance. *Diabetes* 2007;56:285–294. <https://doi.org/10.2337/DB06-0436>.
- [42] Ma Y, Cui D, Zhang Y, et al. Insulin-like growth factor binding protein-2 promotes proliferation and predicts poor prognosis in hepatocellular carcinoma. *OncoTargets Ther* 2020;13:5083–5092. <https://doi.org/10.2147/OTT.S249527>.
- [43] Stanley TL, Fourman LT, Zheng I, et al. Relationship of IGF-1 and IGF-binding proteins to disease severity and glycemia in nonalcoholic fatty liver disease. *J Clin Endocrinol Metab* 2021;106:E520–E533. <https://doi.org/10.1210/CLINEM/DGAA792>.

Keywords: MASLD; SLD; IMID; advanced fibrosis; transcriptome.

Received 3 November 2023; received in revised form 28 June 2024; accepted 2 July 2024; Available online 8 July 2024